



## Precise measurement of intradermal fluid delivery using a low activity technetium-99m pertechnetate tracer

Sahan A. Ranamukhaarachchi<sup>a,b,1</sup>, Tullio V. Esposito<sup>b,1</sup>, Mehrsa Raeiszadeh<sup>a</sup>, Urs O. Häfeli<sup>b</sup>, Boris Stoeber<sup>a,c,\*</sup>

<sup>a</sup> Department of Electrical and Computer Engineering, University of British Columbia, Vancouver, BC V6T 1Z4, Canada

<sup>b</sup> Faculty of Pharmaceutical Sciences, University of British Columbia, Vancouver, BC V6T 1Z3, Canada

<sup>c</sup> Department of Mechanical Engineering, University of British Columbia, Vancouver, BC V6T 1Z4, Canada

### ARTICLE INFO

#### Article history:

Received 30 July 2019

Received in revised form 17 September 2019

Accepted 24 September 2019

Available online 3 October 2019

#### Keywords:

Hollow microneedles

Intradermal delivery

Fluid delivery efficiency

Fluid backflow

Technetium-99m pertechnetate

Radiotracer

### ABSTRACT

A method was developed and validated to determine the intradermal (ID) fluid delivery potential of several ID devices, including hollow microneedles. The novel method used water soluble technetium-99m pertechnetate ( $^{99m}\text{TcO}_4^-$ ) diluted in normal saline to measure the volume of fluid delivered to and remaining in the skin. The fluid that back-flowed to the skin surface and the fluid left on the device surface were also quantified, thus capturing all fluid volumes deposited during intradermal injections. The technique described in this manuscript was used to assess the injection performance of conventional hypodermic needles and hollow microneedles *ex vivo* using porcine skin and *in vivo* with a rat model. Since only a small fraction, 1.1%, of the water-soluble tracer remained bound to the skin when applied topically, the technique can be used to differentiate between injected fluid and backflow. Counting of gamma radiation from  $^{99m}\text{TcO}_4^-$  provided sub-nanoliter resolution for volume measurements, making the proposed method powerful, sensitive, and suitable for the assessments of ID injection devices, particularly for vaccine delivery.

© 2019 Elsevier Ltd. All rights reserved.

### 1. Introduction

Owing to the growth of the area of intradermal (ID) drug delivery, novel medical devices and strategies have been developed, as described by Weniger and Papania [1]. ID delivery of medicines has been explored in depth over the past decade, particularly for vaccines, in order to exploit the high density of immune cells found within the skin [2,3]. In particular, microneedle technologies are promising tools to accurately deliver vaccines and therapeutics into the skin, particularly those that benefit from accessing the immune system and the lymphatic system [4]. Compared with dissolvable microneedles and microneedles with a dissolvable coating containing the drug to be delivered, hollow microneedles do not require re-formulation of active pharmaceutical ingredients and allow a larger therapeutic payload to be delivered into the skin [5]. However, accurately quantifying the small amounts of fluid delivered using microneedles remains a technical challenge.

The performance of ID devices during the delivery of liquid formulations into the skin is assessed for dose accuracy and fluid wastage. The latter is typically assessed as backflow, the leakage of fluid from the injection site back onto the surface of the skin due to the skin's resistance to expansion [6,7]. In the past, gravimetric, volumetric, and several imaging techniques have been used to assess ID fluid delivery during product development [6–9]. Gravimetric analysis has been the go-to method used to determine dose accuracy (fluid delivery potential), fluid wastage, and syringe/ID device dead-space according to ISO 7886-1:1993 and ISO 11608-1:2000 standards published by the International Standards Organization (ISO) [10]. Gravimetric analysis has yielded relatively higher accuracy measurements of fluid delivery using hypodermic needle/syringe devices compared to volumetric analysis [8]. During gravimetric analysis, the delivery device is weighed without filling the fluid, after filling and priming the fluid, and after injecting the fluid into the skin [8]. The difference in the mass of the syringe before and after the injection provides the mass of fluid delivered into the skin, which can be converted to volume of fluid delivered to determine the dose accuracy [8]. However, for ID product development, the gravimetric method provides a number of challenges measuring the typical small delivery volumes, including

\* Corresponding author at: 2054-6250 Applied Science Lane, The University of British Columbia, Vancouver, B.C. V6T 1Z4, Canada.

E-mail address: [boris.stoeber@ubc.ca](mailto:boris.stoeber@ubc.ca) (B. Stoeber).

<sup>1</sup> These authors contributed equally.

lack of measurement sensitivity, evaporation of fluid prior to measurement and the inability to accurately capture fluid backflow as interfering liquids on the surface of the skin, such as oil and sweat, can contribute to errors in measurement [11,12]. Electronic balances are used for measurement of mass of the syringe at various time points during dose accuracy determinations with a typical accuracy of 0.0001 g, corresponding to 0.1  $\mu\text{L}$  accuracy for water [12]. For dead-space determination in hypodermic syringes according to ISO 7886:1 1993, the gravimetric measurement capability requirements are even weaker with listed sensitivity being 0.2 g (200  $\mu\text{L}$ ) at an accuracy of 7 mg (7  $\mu\text{L}$ ). Therefore, an alternative, highly sensitive method for characterizing ID fluid delivery is needed.

Several imaging techniques that are described below have been used to assess, characterize, and quantify fluid flow during ID fluid delivery, but they are inferior in performance to the gravimetric analysis. Injection of X-ray contrast media into the skin using ID delivery techniques, capture of top-view images of the skin at the injection site with an X-ray camera, followed by categorical assessment of the resulting X-ray images based on a clinical scoring scale have been used previously to determine the delivery location of fluid into the skin [7]. The X-ray imaging mechanism did not provide direct measurements of the volume of the fluid delivered and fluid backflow. Laser scanning confocal microscopy (LSCM) has been used for visualization of the skin [13] and quantification of intradermal injections [6], but with significant drawbacks. These drawbacks of LSCM include limited range of lasers to excite fluorophores, requirement of high intensity lasers to penetrate into desired depths of skin for imaging, photo-bleaching of fluorophores and destruction of viable tissues due to exposure to high intensity laser, and auto-fluorescence of skin [13]. Thus, performing quantitative fluid flow assessments from ID injections in the skin using LSCM has not been a feasible technique. A three-dimension ultrasound echography method has been used to determine and locate fluid depositions in the skin using ID delivery techniques [7], but was not a high sensitivity method for fluid flow quantification, due to the low resolution nature of ultrasound imaging [14]. The ultrasound echography method provided bleb and fluid flow profiles within the skin layers, alongside histology cross-sections.

A more powerful methodology involving coating a radio-labelled tracer protein ( $^{14}\text{C}$ -ovalbumin) to the payload of a solid microneedle array was explored by Pearson et al. [15]. The use of  $^{14}\text{C}$ -ovalbumin allowed accurate measurement of the payload delivered to the skin and left on the solid, coated microneedle array; however, this method was only suitable for use with solid matrices, and not with the injection of liquid formulations.

The objectives of this study were to develop an ID fluid delivery characterization technique using a  $^{99\text{m}}\text{TcO}_4^-$  radiotracer and to determine the fluid delivery potential into the skin with several ID delivery devices. The proposed characterization method was tested in *ex vivo* and *in vivo* models and for the ID delivery route only. The proposed characterization was not evaluated for other routes of drug administration, such as intravenous and subcutaneous routes.

## 2. Materials and methods

### 2.1. Injection preparation

A number of methods and devices were assessed for their ID fluid delivery capacity: the Mantoux technique using a 31-gauge needle (31G; BD Ultra-Fine™ short pen needle; 31-gauge, 8 mm; product no. 320109, Becton, Dickinson and Company, Franklin Lakes, NJ, USA), a 26-gauge ID bevel needle (26G; BD Precision-

Glide™ needle; 26-gauge, 9.53 mm; product no. 305110; Becton, Dickinson and Company, Franklin Lakes, NJ, USA); and a single hollow metallic microneedle (ML1) and a 3x2 hollow metallic microneedle array (ML6) devices mounted to a female Luer adapter (0.6 mm height; Microdermics Inc., Vancouver, BC, Canada). The ML1 and ML6 devices were fabricated according to Mansoor et al. [16], and they were inserted along a direction perpendicular to the skin surface using a custom spring-loaded applicator (Microdermics Inc., Vancouver, BC, Canada).

The radioisotope technetium-99 m pertechnetate ( $^{99\text{m}}\text{TcO}_4^-$ ) with a half-life of 6 h was used to evaluate the ID fluid delivery performance of aforementioned methods/devices. The  $^{99\text{m}}\text{TcO}_4^-$  was obtained from the Vancouver General Hospital and diluted in 9 mg  $\text{mL}^{-1}$  sodium chloride (Hospira, Lake Forest, IL, USA) to 740 kBq  $\text{mL}^{-1}$  using a CRC-55tR dose calibrator (Capintec, Florham Park, NJ, USA). This diluted solution is herewith referred to as the  $^{99\text{m}}\text{TcO}_4^-$  solution. During *in vivo* injections, a green tattoo ink (Millennium Colorworks Inc., New York, NY, USA) was incorporated into the  $^{99\text{m}}\text{TcO}_4^-$  solution to aid injection visualization. The ID injection devices to be tested were attached via a Luer connector to a 1 mL BD syringe (product no. 309628, Becton, Dickinson and Company, Franklin Lakes, NJ, USA) containing 0.2–0.4 mL of the  $^{99\text{m}}\text{TcO}_4^-$  solution and primed before injection. Prior to each ID injection, the level of radioactivity in the syringe was measured at a defined time point ( $t_0$ ), providing a radioactivity per volume measurement to start an injection test. The time of the radioactivity measurement was used for decay-correction of the radioactivity per volume value for each injection test at the time of obtaining downstream radioactivity measurements ( $t_1$ ) of the skin sample and swabs, as described later.

### 2.2. Ex vivo skin injections

The use of animal skin *ex vivo* for this study was approved by the University of British Columbia's Animal Care Committee and Biosafety Committee. Freshly excised skin from the abdomen of female miniature Yucatan pigs weighing 20–30 kg (Sinclair Bio-resources, Columbia, MO, USA) was immediately frozen at  $-80^\circ\text{C}$  for 48 h, and thawed for 1 h before testing. Porcine skin samples were stretched and mounted on a support structure according to Ranamukhaarachchi et al. [17,18], where it was previously shown to be mechanically similar to human skin.

Injection of 0.1 mL  $^{99\text{m}}\text{TcO}_4^-$  solution was performed using the ID delivery devices in 4–6 porcine skin samples per device to assess the fluid delivery efficiency (Fig. 1A). As a control, 0.1 mL of the  $^{99\text{m}}\text{TcO}_4^-$  solution was applied topically to the skin using a 20–200  $\mu\text{L}$  micropipette (PIPETTEMAN Classic™, product no. F123601; Gilson Inc., Middleton, WI, USA). Prior to injection or topical fluid application, the weight of the needle-syringe injection device or the pipette was measured on a B120S balance (Sartorius GmbH, Göttingen, Germany). The 31G and 26G needles (according to the Mantoux method [19]) and microneedle devices (according to manufacturer instructions) were inserted into the skin by a person trained in these injections, followed by manual delivery of 0.1 mL  $^{99\text{m}}\text{TcO}_4^-$  solution under 10 s. The ML6 device was also assessed for delivery of a larger volume of  $^{99\text{m}}\text{TcO}_4^-$  solution (0.3 mL  $^{99\text{m}}\text{TcO}_4^-$  solution under 30 s) to determine the performance differences as the fluid delivery target volume increased.

Post-administration, the needle-syringe injection devices were removed from the skin and weighed to determine the net mass released. The net mass was converted to net volume released using the density of normal saline ( $\rho_{\text{saline}} = 1.005 \text{ mg } \mu\text{L}^{-1}$ ). This gravimetric measurement was compared to the total radioactivity released from the syringe for validation of the method. The skin surface was wiped using a series of cotton swabs, as illustrated in Fig. 1B, to collect and capture any  $^{99\text{m}}\text{TcO}_4^-$  solution that

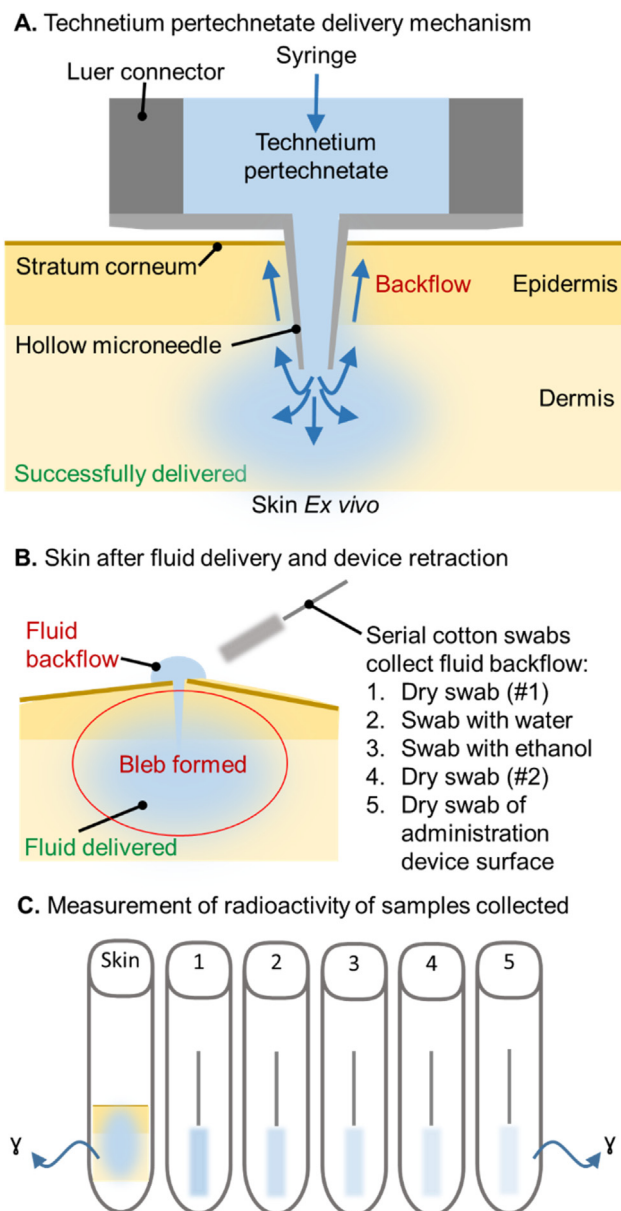


**Fig. 1.** Fluid delivery and measurement methodology. (A) A highly dilute  $^{99m}\text{TcO}_4^-$  solution is administered using ID delivery devices. (B) Fluid backflow to the skin surface from the bleb formed post fluid administration is captured by cotton swabs. (C) Gamma radiation present in skin and cotton swabs is measured using a gamma counter.

back-flowed to the surface of the skin during or after the injection. Since  $^{99m}\text{TcO}_4^-$  is water- and ethanol-soluble, the initial dry swab was followed by a swab dipped in water, a swab dipped in 70 vol % ethanol, and a second dry swab to ensure that no radiotracer was present on the surface of the skin. Another swab was used to collect the  $^{99m}\text{TcO}_4^-$  remaining on the surface of the needle device. All swabs were transferred to plastic test tubes for measurement in an automatic gamma counter (2470 WIZARD<sup>2</sup>, Perkin Elmer, Waltham, MA, USA; minimum detectable concentration is 0.016 kBq and linear detection range for  $^{99m}\text{TcO}_4^-$  is 0.016–294 kBq) as shown in Fig. 1C. The skin sample was released from its support structure and transferred to a plastic test tube for measurement in the gamma counter, as well.

All radioactivity measurements were background-subtracted by the automatic gamma counter and the dose calibrator. As a result

of collecting all avenues of fluid distribution and their respective radioactivity levels during an ID injection, using different batches of  $^{99m}\text{TcO}_4^-$  solutions did not compromise comparability of the characterization method across all devices used in this study. However, for this method to be successful, obtaining a measurement of the radioactivity per volume of the  $^{99m}\text{TcO}_4^-$  solution before each injection was paramount, along with the time of measurement ( $t_0$ ). This is because the automatic gamma counter measurements occurred at a later time point ( $t_1$ ) in the study (while the radioactivity of the  $^{99m}\text{TcO}_4^-$  solution continued to decay), and a time-decay corrected measurement of the radioactivity per volume of the  $^{99m}\text{TcO}_4^-$  solution was needed (at  $t_1$ ) to convert radioactivity in various samples (i.e., skin) to injection volumes.

### 2.3. In vivo skin injections

ID injections were performed on Sprague Dawley rats (Charles River Laboratories, Sherbrooke, QC, Canada) under general anesthesia using the ML1 single microneedle device with a spring-loaded applicator at the Center for Comparative Medicine at the University of British Columbia. The experiments were conducted under the approved protocol A12-0172 by the University of British Columbia's Animal Care Committee. The skin on the dorsal surface of the rat was shaved and then treated with a depilatory cream (Nair; Church & Dwight Co. Inc., Trenton, NJ, USA). A dorsal skin fold was stretched over a plastic vial cap to provide a rigid support to facilitate the microneedle insertion. The ML1 device was connected to a BD 1 mL syringe containing the  $^{99m}\text{TcO}_4^-$  solution mixed with green tattoo ink, and 0.1 mL of the fluid was injected manually in under 10 s at each of three separate sites on the rat. Similarly, 0.3 mL of the fluid solution was injected manually in under 30 s at each of three separate sites on the rat, as well. Backflow on the surface of the skin and ML1 device were removed using swabs as described above. All fluid injection sites were outlined using a permanent marker, photographed and removed by deep excision to the fascia. The excised injection sites and backflow swabs were placed in plastic test tubes and measured in the gamma counter as described above.

### 2.4. Measurement and data analysis

All test tubes were placed in the gamma counter and measured for 30 s in triplicate. The readout from the gamma counter in cpm was converted to SI units (kBq) using a calibration factor (51,600 cpm per kBq). Radioactivity from the skin ( $A_{\text{Skin}}$ ) provided a precise measurement of all fluid that successfully entered the skin, while radioactivity from the cotton swabs ( $A_{\text{Backflow}}$ , test tubes 1–5 in Fig. 1C) provided a measurement of all fluid that was expelled from the syringe but did not remain in the skin (backflow). The absolute total volume delivered ( $V_{\text{Total}}$ ,  $\mu\text{L}$ ) from the syringe was calculated by dividing the sum of radioactivity measurements ( $A_{\text{Total}}$ ) from all test tubes in Fig. 1C by the measured radioactivity per volume of  $^{99m}\text{TcO}_4^-$  solution prior to each injection. For comparison, the total volume delivered from the syringe was also determined by a gravimetric measurement. The ratio of the radioactivity measurements in kBq combined with the total volume delivered provided direct and precise measurements of volume successfully delivered to the skin (Eq. (1)) and backflow volume (Eq. (2))

$$V_{\text{Skin}} = \left( \frac{A_{\text{Skin}}}{A_{\text{Total}}} \right) \times V_{\text{Total}} \quad (1)$$

$$V_{\text{Backflow}} = \left( \frac{A_{\text{Backflow}}}{A_{\text{Total}}} \right) \times V_{\text{Total}} \quad (2)$$

The volume delivered to the skin as a percentage of total volume released from the syringe (Eq. (3)) and the relative volume back-flowed (Eq. (4)) were calculated for each ID delivery device to compare the delivery efficiencies.

$$\%V_{Skin} = \left( \frac{V_{Skin}}{V_{Total}} \right) \times 100 \quad (3)$$

$$\%V_{Backflow} = \left( \frac{V_{Backflow}}{V_{Total}} \right) \times 100 \quad (4)$$

### 3. Results and discussion

#### 3.1. Device performance *ex vivo*

The injection performance of the ID delivery devices and topical control for the *ex vivo* tests are presented in Fig. 2 and in more detail in Table 1. The control, where a 0.1 mL droplet of the  $^{99m}\text{TcO}_4^-$  solution was topically applied to the skin surface, showed that only  $1.1 \pm 0.4\%$  of fluid was left on or adhered to the skin surface. The ability to remove 98.9% of the fluid from the skin surface using the swabbing technique described in Fig. 1B showed that the remaining  $^{99m}\text{TcO}_4^-$  adhering to the skin surface was negligible compared to the volume in the skin or volume removed by swabs. The ML6 microneedle device yielded the highest fluid delivery efficiency with  $92.9 \pm 6.0\%$  of the total fluid released from the syringe reservoir, followed by the 31G needle at  $88.6 \pm 9.5\%$ . The lowest delivery efficiency was reported by the 26G needle at  $68.7 \pm 1.7\%$ , which was significantly different from the ML6 ( $P < 0.001$ ) and 31G ( $P < 0.002$ ) devices at a 95% confidence interval using a two-sample *t*-test. This low delivery efficiency by the 26G needle, which is the conventionally used ID delivery device in clinical settings, may be attributed to the larger fluid backflow path that is created during the insertion and retraction of the needle to and from the skin, allowing fluid to flow back out of the skin more easily to relieve the pressure built up inside the dermis.

The fraction of fluid backflow to the surface of the skin after administration is shown in Fig. 2. The ML6 device ( $7.1 \pm 6.0\%$ ) and the 31G needle ( $11.4 \pm 9.5\%$ ) yielded significantly lower fluid backflow to the surface compared to the 26G needle ( $31.3 \pm 1.7\%$ ) at a 95% confidence interval. It was suspected that delivery of fluid deeper into the reticular dermis with conventional hypodermic needles due to their higher length may allow more accurate volume injections with less fluid backflow, compared to shallower injections into the papillary dermis with microneedles. This was predominantly due to the superior ability of the reticular dermis to accommodate and expand with the incoming fluid in its hydrogel-like, elastic structure compared to the upper papillary dermis [20]. However, shallower intradermal injections using the ML6 device yielding more accurate dermal injections with less fluid backflow refuted that hypothesis.

A higher target fluid delivery volume of 0.3 mL was tested in excised porcine skin with the ML6 device, resulting in a decrease in the delivery efficiency from 92.9% to 86.1% compared to delivery of 0.1 mL, and an increase in the fluid backflow from 7.1% to 13.9%. The decrease in the fluid delivery efficiency most likely arose due to limitations in the fluid absorption by the dermal layer of the skin and the skin's capability to seal off the injection site against the high pressure built up underneath the skin [6]. It was likely that the excised skin had undergone mechanical and structural changes, since it was previously frozen [17], which may have affected the fluid delivery efficiency for larger delivery volumes, compared to intact skin. Injections *in vivo* into live skin may improve the delivery efficiency due to higher elasticity of skin layers, such as the stratum corneum of porcine skin, and blood flow in

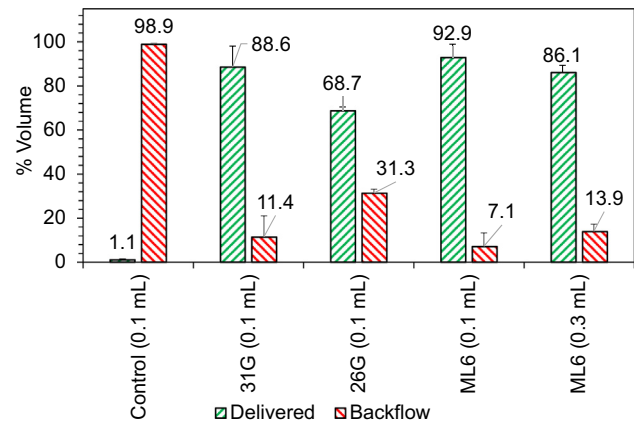


Fig. 2. Comparison of ID fluid delivery methods for successful fluid delivery and fluid backflow resulting in wastage;  $n = 5$  for the control, 31G needle, and 26G needle for 0.1 mL injections;  $n = 6$  for 0.1 mL injections using ML6;  $n = 4$  for 0.3 mL injections using ML6; error bars represent standard deviation.

the dermis. Nonetheless, the volume delivery efficiency with the ML6 device suggested that *ex vivo* porcine skin was able to accommodate 0.3 mL volumes of fluid with dosing accuracies that comply with ISO 11608-1:2000 standard that requires at least 80% fluid delivery efficiency [12].

#### 3.2. Device performance *in vivo*

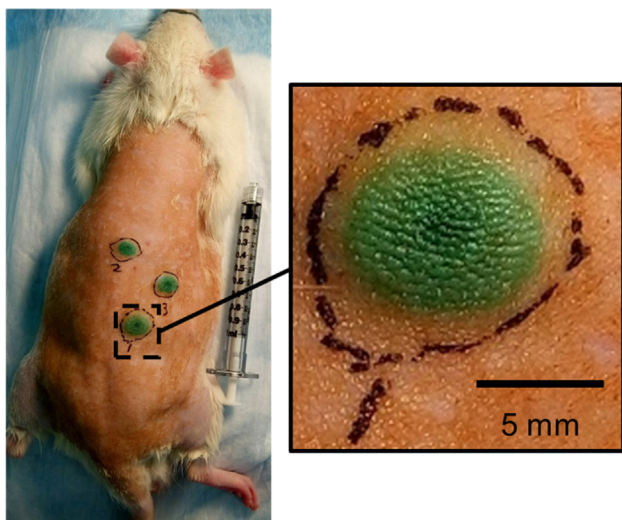
The *in vivo* injection performance of the ML1 device was assessed in a Sprague Dawley rat with the  $^{99m}\text{TcO}_4^-$  solution to determine the fluid delivery efficiency (Fig. 3) with 0.1 mL and 0.3 mL injection volumes. The green tattoo ink mixed into the  $^{99m}\text{TcO}_4^-$  solution clearly helped to visualize the injection site and the bleb formation. It was confirmed that the green tattoo ink did not interact with the  $^{99m}\text{TcO}_4^-$  to negatively affect the gamma radiation readout in samples with known radioactivity levels (data not shown), prior to being utilized in ID injections. Quantification of the amount of radioactivity in the injection sites post-excision showed a 92.5% fluid delivery efficiency and a 7.5% backflow for the 0.1 mL volume. An improvement between *ex vivo* injections in porcine skin and *in vivo* injections in rat skin was not seen for 0.1 mL injections. However, injections of 0.3 mL *in vivo* yielded an improved delivery efficiency of 94.4% and backflow of 5.6%, compared to *ex vivo* porcine skin injections. This improvement was possibly attributed in part to the mechanical properties of *in vivo* rat skin that allowed the skin to expand during fluid delivery more easily, possibly due to higher elasticity. The other reason for the improved fluid delivery efficiency was likely the use of a single hollow microneedle projection *in vivo*, compared to six projections *ex vivo*. When six projections were used *ex vivo*, six micro-pores were created on the skin, which likely provided more paths for fluid backflow to the surface. Whereas, fluid could only backflow through one micro-pore during injection using a single microneedle, thereby potentially maximizing the fluid delivery efficiency. The effect of microneedle array size on the fluid delivery efficiency and backflow will need to be characterized in future studies.

A limitation in this study is the utility of *ex vivo* porcine skin and *in vivo* rat skin to perform the ID injections, rather than *in vivo* human skin, when the final, practically relevant application is for human use. Both porcine skin and rat skin are well-characterized and widely used as comparable animal skin models to human skin. It is anticipated that using intact *in vivo* human skin, instead of frozen porcine skin and fresh rat skin, to conduct the injections performed in this study could yield higher fluid delivery efficiency

**Table 1**  
Comparison of volume delivery efficiency of intradermal delivery devices. Each injection into ex vivo porcine skin using the topical control, 31G needle, 26G needle, and the ML6 device was captured by radioactivity measurements (cpm and kBq units) of fluid delivered to the skin and fluid backflow. The mass released by the syringe was gravimetrically measured as a comparison to the radioactivity measurements.

Intradermal Delivery Method	N	Skin	Volume released from syringe		Radioactivity Measurements						Radioactive Volume Delivered		% Difference	% Radioactive Volume		% Radioactive Volume Delivered Mean ± SD	% Radioactive Volume Backflow Mean ± SD		
			Intended volume (μL)	Gravimetric Measure (mg)	Skin (cpm)	Backflow (cpm)	Total Activity (cpm)	Skin (kBq)	Backflow (kBq)	Activity per Volume (kBq μL <sup>-1</sup> )	Skin (μL)	Backflow (μL)		Skin	Backflow				
Topical application (pipette)	1	Porcine, ex vivo	100	102.7	4814	523,343	528,157	0.94	102.62	1.02	0.93	101.07	-0.7%	0.91	99.09	1.1 ± 0.4	98.9 ± 0.4		
	2		99.1	3002	500,257	503,259	0.59	98.09	1.00	0.59	98.41	-0.1%	0.60	99.40					
	3		101.1	4401	514,644	519,045	0.86	100.91	1.01	0.86	100.14	-0.1%	0.85	99.15					
	4		90.3	9693	588,164	597,858	1.90	115.33	1.30	1.46	88.54	-0.3%	1.62	98.38					
	5		98.8	7024	468,810	475,834	1.38	91.92	0.95	1.45	96.55	-0.8%	1.48	98.52					
31G ID Mantoux	1	Porcine, ex vivo	100	100.6	433,547	16,853	450,400	85.01	3.30	0.87	97.22	3.78	0.4%	96.26	3.74	88.6 ± 9.5	11.4 ± 9.5		
	2		78.4	421,012	47,738	468,749	82.55	9.36	1.18	70.06	7.94	-0.5%	89.82	10.18					
	3		93.6	418,965	119,438	538,402	82.15	23.42	1.14	72.37	20.63	-0.6%	77.82	22.18					
	4		104.9	196,318	1950	198,268	38.49	0.38	0.37	102.98	1.02	-0.9%	99.02	0.98					
	5		99.2	142,448	35,737	178,185	27.93	7.01	0.35	78.82	19.78	-0.6%	79.94	20.06					
26G ID Mantoux	1	Porcine, ex vivo	100	123.4	2,183,470	1,142,683	3,326,153	42.81	22.41	0.53	81.07	42.43	0.1%	65.65	34.35	68.7 ± 1.7	31.3 ± 1.7		
	2		87.8	1,790,398	809,802	2,600,200	35.11	15.88	0.58	60.59	27.41	0.2%	68.86	31.14					
	3		118.7	2,486,423	1,082,542	3,568,965	48.75	21.23	0.59	82.90	36.10	0.3%	69.67	30.33					
	4		105.5	1,235,135	539,517	1,774,652	24.22	10.58	0.33	73.91	32.29	0.7%	69.60	30.40					
	5		96.9	1,548,399	673,475	2,221,874	30.36	13.21	0.45	67.04	29.16	-0.7%	69.69	30.31					
ML6	1	Porcine, ex vivo	100	126.8	411,840	89,755	501,594	80.75	17.60	0.78	103.75	22.61	-0.3%	82.11	17.89	92.9 ± 6.0	7.1 ± 6.0		
	2		101.4	441,870	26,423	468,293	86.64	5.18	0.91	94.83	5.67	-0.9%	94.36	5.64					
	3		119.6	468,682	12,739	481,421	91.90	2.50	0.78	117.12	3.18	0.6%	97.35	2.65					
	4		104.6	404,932	6429	411,361	79.40	1.26	0.77	103.36	1.64	0.4%	98.44	1.56					
	5		97.7	381,547	19,519	401,066	74.81	3.83	0.81	92.18	4.72	-0.8%	95.13	4.87					
	6		126.5	465,297	52,081	517,378	91.23	10.21	0.80	113.35	12.69	-0.4%	89.93	10.07					
	7		300	317.2	1,077,858	148,598	1,226,456	211.34	29.14	0.76	279.03	38.47	0.1%	87.88	12.12			86.1 ± 3.2	13.9 ± 3.2
	8		315.1	1,057,624	239,607	1,297,232	207.38	46.98	0.81	257.55	58.35	0.3%	81.53	18.47					
	9		311.9	1,105,820	139,491	1,245,311	216.83	27.35	0.78	277.32	34.98	0.1%	88.80	11.20					
	10		288.5	1,031,274	166,168	1,197,442	202.21	32.58	0.81	249.07	40.13	0.2%	86.12	13.88					

### A. *In vivo* injection of $^{99m}\text{Tc}$ solution using ML1 hollow microneedle device



### B. *In vivo* fluid delivery profile in Sprague Dawley rats

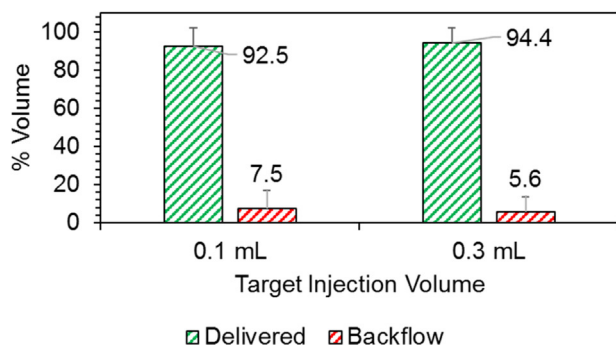


**Fig. 3.** *In vivo* delivery of  $^{99m}\text{Tc}$  solution using the ML1 single microneedle device in Sprague Dawley rats ( $n = 3$  for the 0.1 mL injections;  $n = 3$  for 0.3 mL injections; error bars represent standard deviation).

and reduced backflow due to mechanical intactness of the skin and higher elasticity, and remains to be examined further.

### 3.3. Comparison of methodologies

The performance of this  $^{99m}\text{TcO}_4^-$  injection methodology was significantly superior compared to the conventional gravimetric measurements in many aspects. The sensitivity of the measurement was determined to be  $39,441 \text{ cpm kBq}^{-1}$  from the slope of the  $^{99m}\text{TcO}_4^-$  calibration curve in the gamma counter (data not shown). At this measurement sensitivity, the volume detection sensitivity was significantly higher than gravimetric measurement, and ranged between  $1.29 \times 10^4$  and  $5.14 \times 10^4 \text{ kBq } \mu\text{L}^{-1}$  ( $7.03 \times 10^7$ – $1.41 \times 10^9 \text{ cpm } \mu\text{L}^{-1}$ ). The volume detection sensitivity was provided as a range since the total activity for each injection varied between 34.8 and 254.4 kBq ( $1.78 \times 10^5$ – $3.57 \times 10^6 \text{ cpm}$ ), as different batches of  $^{99m}\text{TcO}_4^-$  solutions were used to assess each device. The background within the energy window for  $^{99m}\text{Tc}$  ( $140 \pm 28 \text{ keV}$ ) on the gamma counter that was used for measurements herein was  $0.007 \pm 0.002 \text{ kBq}$  ( $35.9 \pm 8.3 \text{ cpm}$ ), and the limit of detection, determined as ten times standard deviation of blank, was determined to be  $0.016 \text{ kBq}$  (83 cpm). Thus, the use of the proposed volume determination method allowed quantifying the fluid volumes as low as  $9.5 \times 10^{-7} \mu\text{L}$  accurately, which is approximately five orders of magnitude lower than what is achievable by the gravimetric method (0.1  $\mu\text{L}$ ).

During gravimetric measurements, the weight of the syringe and connected device is measured during each step of the process, as described previously. Many challenges of the gravimetric method, including lower measurement sensitivity, potential errors caused by fluid evaporation prior to measurement, and the inability to accurately capture fluid backflow have been addressed by the proposed method of evaluating fluid delivery using  $^{99m}\text{TcO}_4^-$  solution. Accurate quantification of fluid backflow has not been addressed to date, due to the difficulty of collecting only the fluid back-flowed, and not any other liquids present on the skin surface, such as sweat, oil and interstitial fluid [11]. With the  $^{99m}\text{TcO}_4^-$  method, the presence of interfering substances did not affect the fluid backflow measurements by the gamma counter.

The total volume released from the syringe during each injection was evaluated by radioactivity and gravimetric measurement. The two methods were comparable and consistent in evaluating the total volume released from the syringe, with less than  $\pm 1\%$  difference between the two methods (Table 1).

The proposed methodology of injecting extremely low activities of  $^{99m}\text{TcO}_4^-$  solution into the skin could be potentially used in clinical settings for dose accuracy determinations of ID and other delivery devices without posing a significant safety risk to the patients or workers. The radiation dose levels employed in this study would already be significantly lower than occupational limits recommended by the International Commission on Radiological Protection (ICRP), Federal Aviation Administration (FAA), and the National Council on Radiation Protection and Measurements (NCRP). Using dosimetric OLINDA/EXM code estimates, an injection of the highest  $^{99m}\text{TcO}_4^-$  activity concentrations used in this study ( $6.29 \text{ MBq mL}^{-1}$ ) and the highest volume injected (300  $\mu\text{L}$ ) would give a full body radiation dose of  $8.15 \mu\text{Sv}$  if the assumption that the radioactivity is distributed equally throughout the system and is not eliminated until complete decay is made (worst case scenario) [21]. This radiation dose is exactly one tenth of the dose that a flight passenger receives from the cosmic radiation during a transatlantic flight at 10,000 m [22]. However, given the extremely high sensitivity and low limit of detection of this methodology for quantifying fluid delivery into skin, the total activity used in a measurement can be significantly reduced, while still achieving far superior measurements compared to the gravimetric method.

## 4. Conclusions

A novel method has been developed to accurately measure fluid volumes during ID delivery of pharmaceutical formulations into the skin to determine fluid delivery efficiency and fluid wastage. The use of aqueous formulations with extremely low activities of  $^{99m}\text{TcO}_4^-$  allowed highly accurate and sensitive determinations of fluid delivery into the skin as well as the fluid backflow onto the skin surface with extremely low limits of detection, compared to the conventional gravimetric method. The new method was assessed in *ex vivo* porcine skin and *in vivo* rat skin. Using  $^{99m}\text{TcO}_4^-$  will allow assessment of ID delivery devices and methodologies in an optimal and fast way to enable the development of more effective, painless, and potentially self-administrable therapies for patients. The method was effective at demonstrating that mechanically bypassing the stratum corneum layer with a minimally invasive device allows successful ID delivery of fluid; and allowing precise comparison between the performances of ID delivery devices.

## Declaration of Competing Interest

The authors declare that they have no known competing financial interests or personal relationships that could have appeared to influence the work reported in this paper.

## Acknowledgement

The authors thank the Center for Comparative Medicine at UBC for providing the excised porcine skin samples for the ex vivo injection assessments; and the Vancouver General Hospital for providing the radioisotopes used in this study. The authors also thank the Vanier Canada Graduate Scholarship program, Canada and the Collaborative Health Research Program (grant ID: CHRP 446570-13) by the Canadian Institute for Health Research, Canada and the Natural Sciences and Engineering Research Council of Canada, Canada for financial contributions towards this research. This research was undertaken, in part, thanks to funding from the Canada Research Chairs program, Canada (file number: 950-228738).

## References

- [1] Weniger BG, Papania MJ. Alternative vaccine delivery methods. In: *Vaccines*. Amsterdam: Elsevier; 2008. p. 1357–92.
- [2] Kendall M. Engineering of needle-free physical methods to target epidermal cells for DNA vaccination. *Vaccine* 2006;24:4651–6.
- [3] Prausnitz MR, Langer R. Transdermal drug delivery. *Nat Biotechnol* 2008;26:1261–8.
- [4] Arora A, Prausnitz MR, Mitragotri S. Micro-scale devices for transdermal drug delivery. *Int J Pharm* 2008;364:227–36.
- [5] van der Maaden K, Trietsch SJ, Kraan H, Varypataki EM, Romeijn S, Zwier R, et al. Novel hollow microneedle technology for depth-controlled microinjection-mediated dermal vaccination: a study with polio vaccine in rats. *Pharm Res* 2014;31:1846–54.
- [6] Mansoor I, Lai J, Ranamukhaarachchi S, Schmitt V, Lambert D, Dutz J, et al. A microneedle-based method for the characterization of diffusion in skin tissue using doxorubicin as a model drug. *Biomed Microdev* 2015;17:1–10.
- [7] Laurent PE, Bonnet S, Alchas P, Regolini P, Mikszta JA, Pettis R, et al. Evaluation of the clinical performance of a new intradermal vaccine administration technique and associated delivery system. *Vaccine* 2007;25:8833–42.
- [8] Poppe LB, Savage SW, Eckel SF. Assessment of final product dosing accuracy when using volumetric technique in the preparation of chemotherapy. *J Oncol Pharm Pract* 2016;22:3–9.
- [9] Krzywon M, van der Burg T, Fuhr U, Schubert-Zsilavec M, Abdel-Tawab M. Study on the dosing accuracy of commonly used disposable insulin pens. *Diab Technol Ther* 2012;14:804–9.
- [10] Luijf Y, DeVries J. Dosing accuracy of insulin pens versus conventional syringes and vials. *Diab Technol Ther* 2010;12:S-73–S-7.
- [11] Laurent P, Pettis R, Easterbrook W, Berube J. Evaluating new hypodermic and intradermal injection devices. *Med Dev Technol* 2006;17:16–9.
- [12] Asakura T, Seino H, Kageyama M, Yohkoh N. Dosing accuracy of two insulin pre-filled pens. *Curr Med Res Opin* 2008;24:1429–34.
- [13] Alvarez-Román R, Naik A, Kalia Y, Fessi H, Guy RH. Visualization of skin penetration using confocal laser scanning microscopy. *Eur J Pharm Biopharm* 2004;58:301–16.
- [14] Schwarz M, Omar M, Buehler A, Aguirre J, Ntziachristos V. Implications of ultrasound frequency in optoacoustic mesoscopy of the skin. *IEEE Trans Med Imag* 2015;34:672–7.
- [15] Pearson FE, McNeilly CL, Crichton ML, Primiero CA, Yukiko SR, Fernando GJ, et al. Dry-coated live viral vector vaccines delivered by nanopatch microprojections retain long-term thermostability and induce transgene-specific T cell responses in mice. *PLoS ONE* 2013;8:e67888.
- [16] Mansoor I, Liu Y, Häfeli U, Stoeber B. Arrays of hollow out-of-plane microneedles made by metal electrodeposition onto solvent cast conductive polymer structures. *J Micromech Microeng* 2013;23:085011.
- [17] Ranamukhaarachchi S, Lehnert S, Ranamukhaarachchi S, Sprenger L, Schneider T, Mansoor I, et al. A micromechanical comparison of human and porcine skin before and after preservation by freezing for medical device development. *Sci Rep* 2016;6.
- [18] Ranamukhaarachchi SA, Schneider T, Lehnert S, Sprenger L, Campbell JR, Mansoor I, et al. Development and validation of an artificial mechanical skin model for the study of interactions between skin and microneedles. *Macromol Mat Eng* 2016;301:306–14.
- [19] Mantoux C. L'intradermo-réaction a la tuberculine et son interprétation clinique. *Presse Medicale* 1910;18:10–3.
- [20] Achterberg VF, Buscemi L, Diekmann H, Smith-Clerc J, Schwengler H, Meister J-J, et al. The nano-scale mechanical properties of the extracellular matrix regulate dermal fibroblast function. *J Invest Dermatol* 2014;134:1862–72.
- [21] Stabin MG, Sparks RB, Crowe E. OLINDA/EXM: the second-generation personal computer software for internal dose assessment in nuclear medicine. *J Nucl Med* 2005;46:1023–7.
- [22] In: England PH, editor. *Ionising radiation: dose comparisons*; 2011.